On the variation of the energy scale 22

An analysis of SPARC galaxies

Thu 26th Nov 2020
(Originally Wed 16th Jan 2019)
www.varensca.com

Summary

The conjecture has been put forward that the energy scale can vary from location to location. This conjecture enables galaxy rotation curves and other astronomical phenomena to be explained without the need for any dark matter. The SPARC catalogue provides rotation curve and mass distribution data for 175 disk galaxies. An analysis of the SPARC data, using energy scale variations, shows that the equation for the expected rotational velocity:

$$\boldsymbol{u^2(r) = \frac{G}{r}\int_{x=0}^{r} dM_e(x)}$$

leads naturally to the following equation for the observed rotational velocity:

$$\boldsymbol{v^2(r) = \frac{G}{r}\int_{x=0}^{r} \left\{\frac{r}{x}\right\}^{\alpha} dM_e(x)}$$

where $\boldsymbol{M_e}$ is the effective mass; the only adjustable parameter is the exponent $\boldsymbol{\alpha}$, which is found to lie in the range $\boldsymbol{+0.5 \leq \alpha \leq +1.8}$. This new equation gives good fits to the observed rotation curves of SPARC galaxies. It follows that there is no requirement for dark matter in disk galaxies.

1 Introduction

1.1 JoKe1 (2015) put forward the conjecture that the energy scale can vary from location to location. It showed that the flat rotation curves of spiral galaxies can be explained by variations in the energy scale, without the need for any dark matter.

1.2 JoKe2 (2015) and JoKe3 (2015) extended the work using an improved model of a Gaussian density distribution for the galaxy and another Gaussian for the energy scale variation. Good fits were obtained for the rotation curves of 74 spiral galaxies. The model worked with just the observed rotation curve and did not take into account any estimates of the actual mass distribution.

1.3 The SPARC catalogue (Lelli et al, 2016) presents both the rotation curve data and the mass distribution data for 175 disk galaxies. This enables a much better examination to be undertaken of the conjecture of energy scale variations. In particular the problem can be inverted to get at the shape of the energy scale variation, which until now has been assumed to have a Gaussian profile.

1.4 We can now construct the observed rotation curve from the baryonic mass distribution alone. We do not have to assume a shape for the density distribution; this is given by the SPARC data. And we do not have to assume a shape for the energy scale variation; this comes from analysing the SPARC data. This paper explains how we arrive at these results.

2 Theoretical considerations

2.1 In this section we look at how energy scale variations can be used to explain the rotation curves of disk galaxies, and how we might examine the form of energy scale variations.

2.2 Newton's law of gravity tells us that the force on mass, m_A, from a central mass, M_0, is

$$m_A \ddot{r} = -\frac{G M_0 m_A}{r^2} \tag{1}$$

where M_0, m_A are the two masses; r the separation; $\ddot{r}$ the acceleration; G the gravitational constant. It follows that the circular velocity, $u(r)$, is given by

$$u^2(r) = \dot{r}^2 = \frac{G M_0}{r} \tag{2}$$

2.3 For a spherically-symmetric distribution of mass, rather than a single point mass, equation (2) becomes

$$u^2(r) = \frac{G}{r} \int_{x=0}^{r} dM(x) \tag{3}$$

where $dM(x)$ is the mass increment of a spherical shell.

2.4 In JoKe1 (2015) we put forward the conjecture that the energy scale can vary from location to location. This leads to equation (1) being replaced by

$$m_A \ddot{r} = -\frac{G M_0 m_A}{r^2} \frac{\xi(0)}{\xi(r)} \tag{4}$$

where ξ is the function of position that describes the energy scale variation; $\xi(0)$ is the value of the function at mass M_0; $\xi(r)$ the value at mass m_A. It then follows that the circular velocity, as given by equation (2), becomes

$$v^2(r) = \frac{G M_0}{r} \frac{\xi(0)}{\xi(r)} \tag{5}$$

where we use $v(r)$ for the velocity with an energy scale variation and $u(r)$ for the velocity with no energy scale variation.

2.5 And for a spherically-symmetric distribution of mass, rather than a single point mass, equation (3) becomes

$$\boldsymbol{v^2(r) = \frac{G}{r}\frac{1}{\xi(r)}\int_{x=0}^{r}\xi(x)\,dM(x)} \qquad (6)$$

2.6 The ξ-function in equation (6) can be thought of as a weighting function (rather than an energy scale variation). Each increment of mass, $\boldsymbol{dM(x)}$, is weighted with the value of the ξ-function, $\boldsymbol{\xi(x)}$, at the increment. The ξ-function is dimensionless and the $\boldsymbol{\xi(r)}$ values are pure numbers.

2.7 If we know the mass distribution, $\boldsymbol{dM(x)}$, and the form of the energy scale variation, $\boldsymbol{\xi(x)}$, then we can calculate the observed rotation speed $\boldsymbol{v(r)}$, using equation (6). This procedure was carried out in JoKe1 (2015) for a central point mass and a Gaussian energy scale variation. It successfully reproduced the observed rotation curves beyond 10kpc for six galaxies. JoKe2 (2015) replaced the point mass with a Gaussian density distribution, which enabled the central region to be fitted as well. JoKe3 (2015) applied this simple model to a sample of 74 spiral galaxies and good fits for the rotation curves were obtained in all cases. In these papers the shapes of the density distribution and energy scale variation were assumed to be Gaussian as there was no observational data to work with.

2.8 Of course, it is important to note that spiral galaxies are not spherically-symmetric. They are disks where the visible matter is distributed not in a sphere but in a thin disk that can be considered to be axisymmetric. The brightness of these disk galaxies falls off exponentially which means, for a constant mass-to-light ratio, that the density also falls off exponentially. So, we need to look at the gravitational attraction of thin exponential disks. This has been covered in detail by Binney & Tremaine (2008) where the differences between a sphere and a disk are made clear. For instance, a point inside a spherical shell experiences no gravitational acceleration whereas a point inside a ring experiences a gravitational acceleration outwards, away from the centre and towards the ring.

2.9 As mentioned above, the brightness of disk galaxies is observed to fall off exponentially

$$\boldsymbol{I(r) = I_o \exp(-r/R_d)} \qquad (7)$$

where $\boldsymbol{I(r)}$ is the intensity; $\boldsymbol{R_d}$ is the characteristic distance, typically ~2 kpc in disk galaxies. It follows that, for a fixed mass-to-light ratio, the surface density, $\boldsymbol{\sigma(r)}$, is given by

$$\boldsymbol{\sigma(r) = \sigma_o \exp(-r/R_d)} \qquad (8)$$

The gravitational potential in the disk, $\varphi(r)$, can be obtained from Poisson's equation (Binney & Tremaine, 2008), and the circular velocity found from

$$u^2(r) = r\frac{\partial \varphi}{\partial r} \tag{9}$$

2.10 If we know the distribution of normal (baryonic) matter across a disk galaxy, then we can get at the gravitational potential by solving Poisson's equation and calculate the expected rotation speed, $u(r)$, through equation (9). The problem facing astronomers is that the expected velocity, $u(r)$, is always less than the observed velocity, $v(r)$. The current solution to this problem is the ad hoc postulate that dark matter exists and that galaxies are embedded in large spherical haloes of dark matter. Dark matter then gives rise to a velocity contribution, $w(r)$, given by

$$w^2(r) = \frac{G}{r}\int_{x=0}^{r} dM_{DM}(x) \tag{10}$$

where $dM_{DM}(x)$ is the mass increment of a spherical shell of dark matter.

2.11 The observed velocity, $v(r)$, is now given by

$$v^2(r) = u^2(r) + w^2(r) \tag{11}$$

Given the expected velocity, $u(r)$, and the observed velocity, $v(r)$, we can always introduce sufficient dark matter that equation (11) holds. Dark matter has no predictive power in the sense that, given the mass distribution, it cannot predict the observed rotation curve. Dark matter is simply a rolling fudge factor added to make equation (11) work. Whatever the observed and expected velocities are, we can always find an amount of dark matter that explains the data.

2.12 Binney & Tremaine (2008) also show that the difference in the circular velocity, between an exponential disk and a sphere with the same mass, is only a few per cent. And this difference becomes rapidly smaller at larger distances from the galaxy centre. This means we can define an 'effective mass' given by

$$u^2(r) = \frac{G}{r}\int_{x=0}^{r} dM_e(x) \tag{12}$$

where $dM_e(x)$ is the effective mass of an increment of the disk (not a spherical shell). So, although in general there can be substantial differences between spheres and disks, these differences are small in the case of an exponential disk.

2.13 It then follows that our equation (6) for the circular velocity in an energy scale variation should be

$$v^2(r) = \frac{G}{r}\frac{1}{\xi(r)}\int_{x=0}^{r}\xi(x)\,dM_e(x) \tag{13}$$

where the increment in the effective mass, $dM_e(x)$, is the same as in equation (12). It should be noted that $v(r)$ is the actual rotational velocity as measured by the observations of disk galaxies.

2.14 **WYSIWYG**: what you see is what you get.
We can look at equation (1) in a different way. The gravitational acceleration is usually given by adding up the contributions from all the masses:

$$\ddot{r} = -\frac{G}{r^2}\left\{M_{gas} + M_{stars} + M_{bulge} + SOM\right\} \tag{14}$$

where SOM stands for "some other (additive) mass", currently interpreted as dark matter. Our equation (4) is different; what we are saying is

$$\ddot{r} = -\frac{G}{r^2}\left\{M_{gas} + M_{stars} + M_{bulge}\right\} \times SOE \tag{15}$$

where SOE stands for "some other (multiplicative) effect". In our case we are calling this other effect a variation in the energy scale. Others may choose to label it differently. The main point is we take the view that there are no other masses, there is no dark matter, and that the matter we observe is all there is.

2.15 The SPARC catalogue of galaxies (Lelli et al, 2016) provides the observed and expected velocities for 175 disk galaxies. The expected velocity is given in the form

$$u^2 = \Upsilon_b\,|u_{bulge}|\,u_{bulge} + |u_{gas}|\,u_{gas} + \Upsilon_s|u_{star}|\,u_{star} \tag{16}$$

where Υ_b is the mass-to-light ratio of the central bulge; Υ_s is the mass-to-light ratio of the disk of stars; u_{bulge} is the contribution to the velocity from the central bulge; u_{gas} is the velocity from the gas; u_{star} is the velocity from the disk of stars. The mass-to-light ratio for the bulge is set to 0.7 by default; the mass-to-light ratio for the disk of stars is set to 0.5 by default.

2.16 We are now in a position where we can examine the form of our ξ-function that describes the variation of the energy scale. Knowing the expected velocity from the SPARC catalogue, we can get at the distribution of normal matter by inverting equation (12). In incremental form this is

$$G\,\Delta\{M_e(r)\} = \Delta\{r\,u^2(r)\} \tag{17}$$

2.17 And knowing the mass distribution we can get at the shape of our ξ-function by inverting equation (13). In incremental form this is

$$\boldsymbol{\xi(r)\, G\, \Delta\{M_e(r)\}} \;=\; \boldsymbol{\Delta\{\xi(r)\, r\, v^2(r)\}} \qquad (18)$$

2.18 At this stage we have no idea what the shape of the ξ-function might be, or whether equation (18) can be solved to give any meaningful values at all. What we have to do is process the data in the SPARC catalogue and see what we end up with. The results of this process are covered in the next section.

3 A sample of SPARC galaxies

3.1 The next few pages show the results of applying the ideas of the previous section to a sample of galaxies from the SPARC catalogue (Lelli et al, 2016). Some are gas dominated, some dominated by the stellar disk, and some have a central bulge.

3.2 The top left panel shows the SPARC data. The black diamonds are the observations of the rotation curve. The purple curve is the contribution to the velocity from the central bulge (if one exists); the orange curve from the disk of stars; the green curve from the gas. The blue curve is the expected velocity given by aggregating the components using equation (16).

3.3 The top right panel shows the cumulative mass distribution corresponding to the velocities in the top left panel. The values are found by solving equation (17), which is the numerical form of equation (12). The black diamonds give the observed total mass corresponding to the black diamonds in the top left panel. The blue line gives the normal matter mass corresponding to the blue line in the top left panel. This diagram shows whether the observed or expected masses are levelling off or are still increasing at the outer edge of the galaxy. The observed mass usually shows a continuing increase; the expected mass usually shows convergence. If the observed mass is interpreted as the expected mass plus the dark matter mass, then we can define the dark matter ratio as

$$\text{Ratio(dark matter)} = \frac{\boldsymbol{M}(\text{dark matter})}{\boldsymbol{M}(\text{observed})} = \frac{\boldsymbol{M}(\text{observed}) - \boldsymbol{M}(\text{expected})}{\boldsymbol{M}(\text{observed})} \qquad (19)$$

3.4 The bottom left panel shows, in logarithmic form, the ξ-function as a function of distance, as derived by solving equation (18), which is the numerical form of equation (13). In practice $\boldsymbol{\xi(r)}$ is found by solving equations (17) and (18). The black diamonds correspond to the observed velocities shown in the top left panel. All galaxies show an approximate linear relation. The red line is a straight line that approximates to the observed data. It turns out that it is only the slope of the red line that is important and not its position. The fitting procedure assumes an average value of ξ=1000 across the first interval.

3.5 The bottom right panel shows the rotation curve again. The black diamonds are the same observed velocities as in the top left panel. Similarly, the blue line is the same expected velocities as in the top left panel. The red line is the fitted rotation curve derived by applying the red line from the bottom left panel for $\boldsymbol{\xi(x)}$ to the blue line from the top right panel for the mass $\boldsymbol{dM_e(x)}$. The fitted velocity is calculated by applying the $\boldsymbol{\xi(x)}$ and $\boldsymbol{dM_e(x)}$ to equation (13).

3.6 Panels for all the SPARC galaxies used in this paper are shown separately in paper JoKe23 (2019).

DDO 161

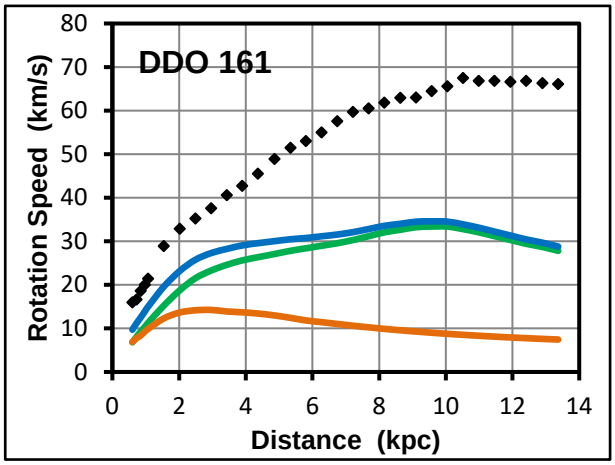

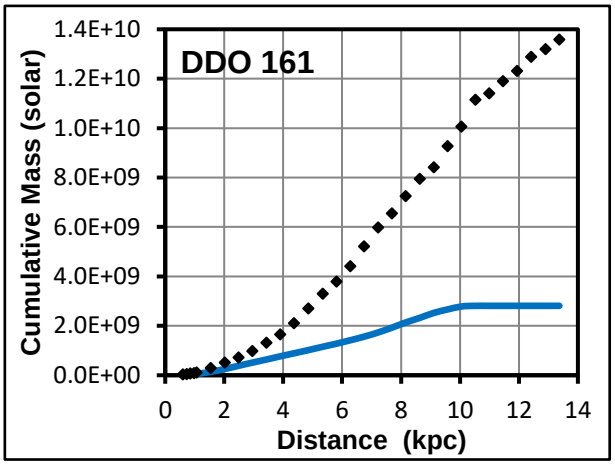

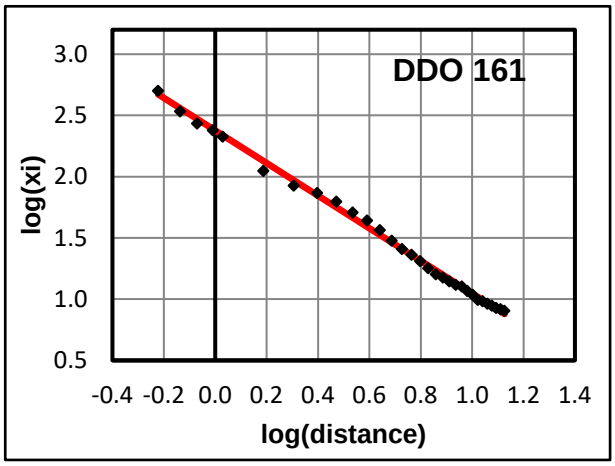

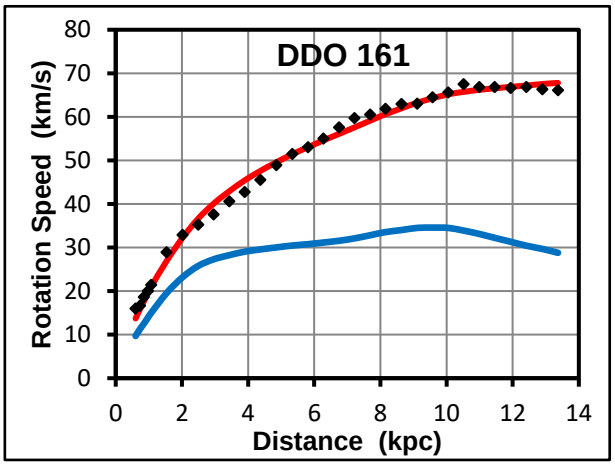

Top left: rotation curve from SPARC data
Top right: cumulative mass, converges by 10 kpc
Bottom left: ξ-function
Bottom right: fitted rotation curve

Fit parameters

ϒ, M-to-L	0.30
ξ, slope	-1.33
DM factor	3.8
Fit quality	good

Comments:
Galaxy is gas rich; gas dominates over stellar disk.

NGC 2403

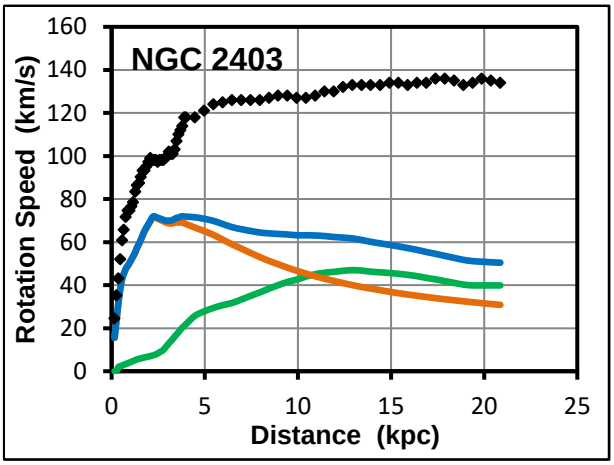

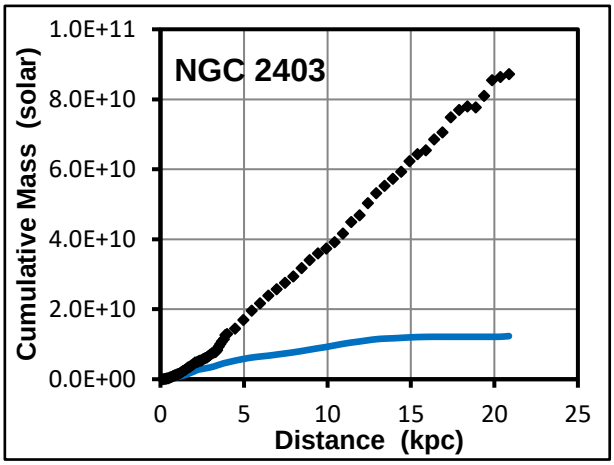

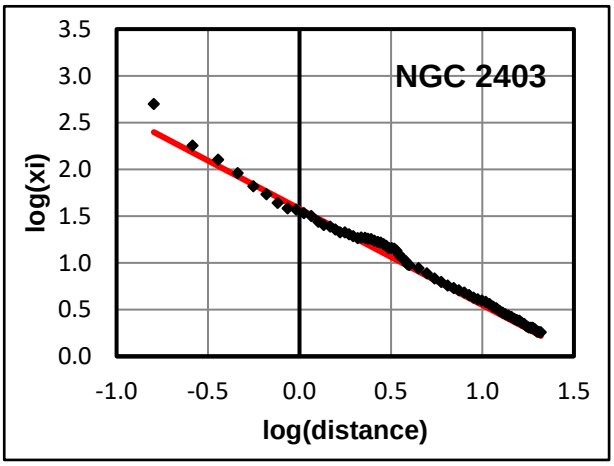

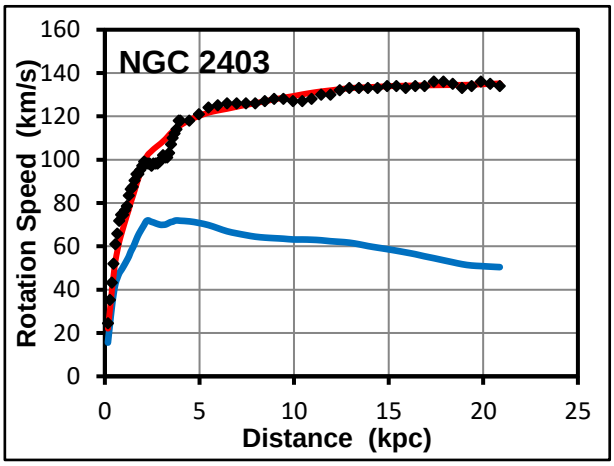

Top left: rotation curve from SPARC data
Top right: cumulative mass from SPARC data
Bottom left: ξ-function
Bottom right: fitted rotation curve

Comments

ϒ, M-to-L	0.45
ξ, slope	-1.02
DM	6.1
quality	good

Red line is a pretty good fit all the way to 21 kpc. There is an obvious deviation around 3 kpc, and a smaller deviation around 10 kpc.

NGC 5033

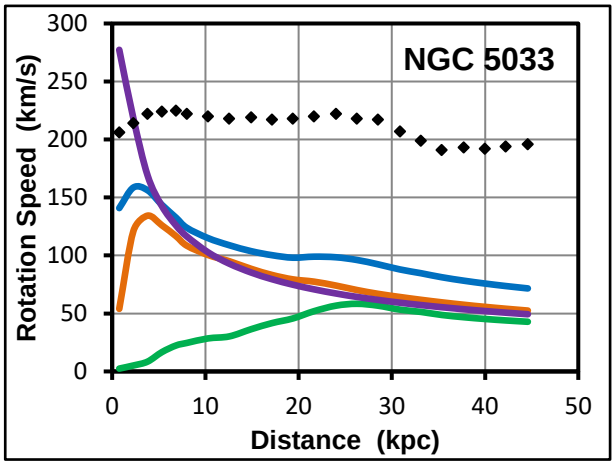

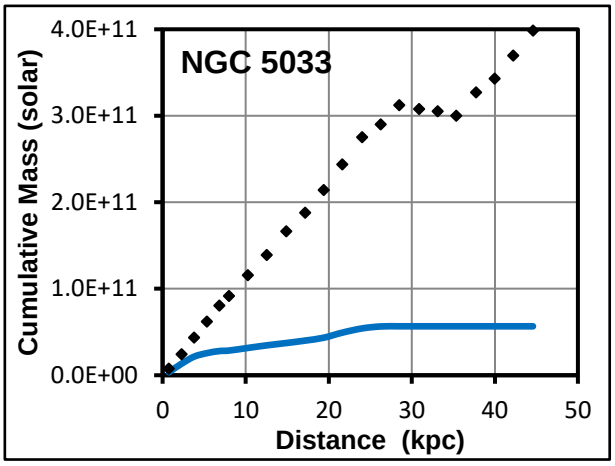

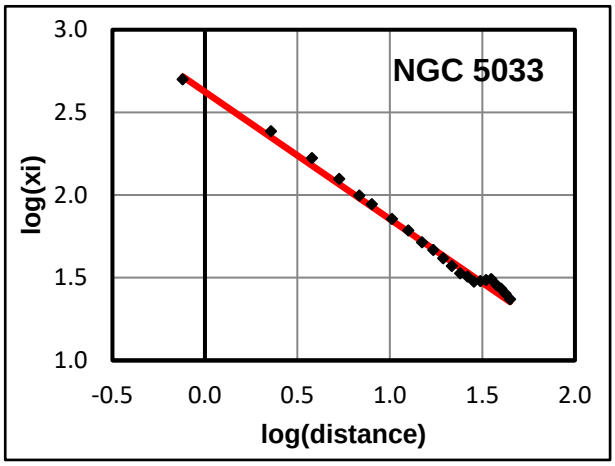

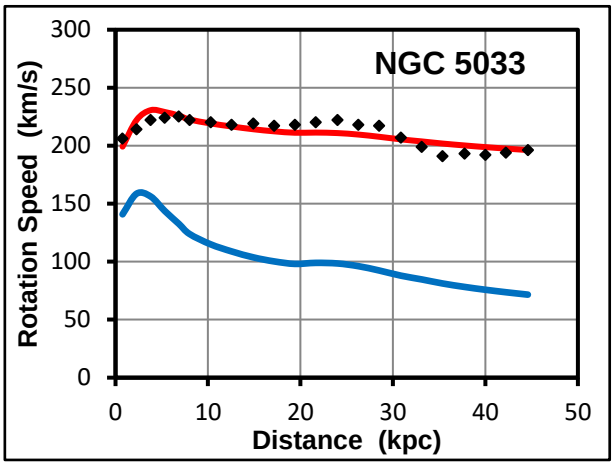

Top left: rotation curve from SPARC data
Top right: cumulative mass
Bottom left: ξ-function
Bottom right: fitted rotation curve

Fit parameters

Bulge, M-to-L	0.22
Disk, M-to-L	0.32
ξ, slope	-0.77
DM factor	6.0
Fit quality	OK

Comments:
Galaxy has a central bulge.

UGC 128

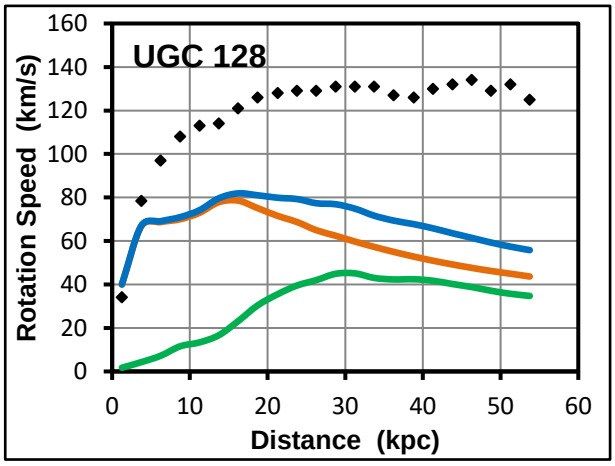

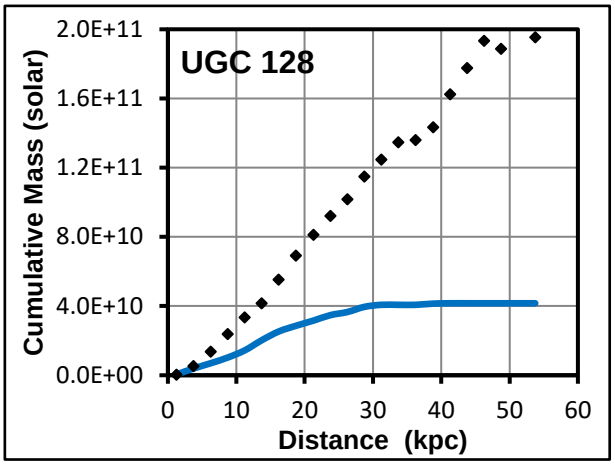

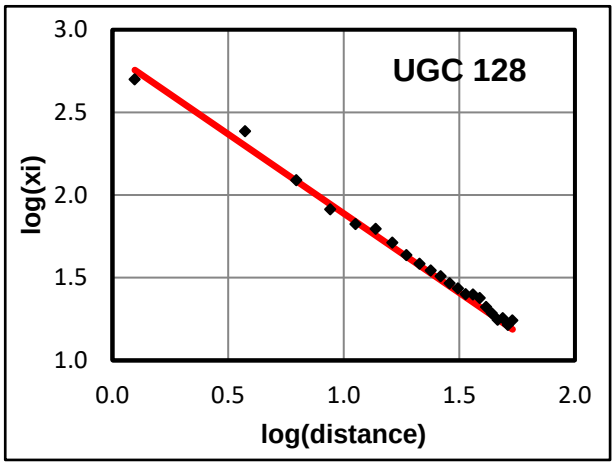

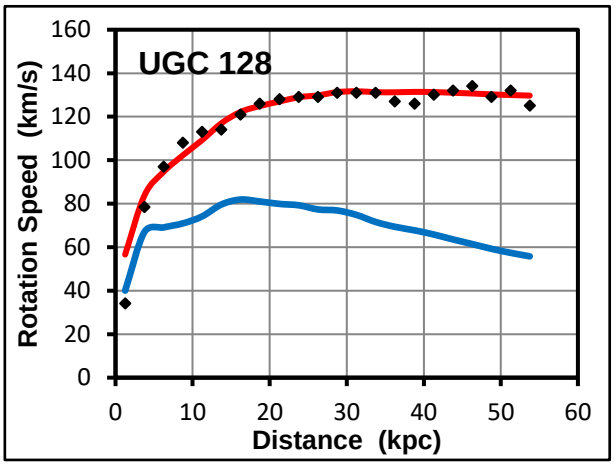

Top left: rotation curve from SPARC data
Top right: cumulative mass
Bottom left: ξ-function
Bottom right: fitted rotation curve

Fit parameters

ϒ, M-to-L	1.85
ξ, slope	-0.96
DM factor	3.7
Fit quality	good

4 A power law relationship

4.1 The surprising result that comes out of the above analysis of SPARC galaxies is that they all show a power law relationship between the $\xi(r)$ function and the radial distance. This is clear from the linear relationships that are apparent in all the bottom left panels. This result is completely unexpected.

4.2 The linear approximation revealed in the bottom left panels does not cover the whole rotation curve. Often the galaxy centre and the outermost parts deviate from a straight line. Also, some galaxies have structure in their rotation curves that also does not fit. Nevertheless, a straight line is a good approximation to the logarithm of the ξ-function.

4.3 In equation (13) we can split the integral into two parts to give:

$$v^2(r) = \frac{G}{r}\frac{1}{\xi(r)}\left\{\int_{x=0}^{r_1}\xi(x)\,dM_e(x) + \int_{x=r_1}^{r}\xi(x)\,dM_e(x)\right\} \quad (20)$$

$$= \frac{G}{r}\frac{1}{\xi(r)}\left\{P(r_1) + \int_{x=r_1}^{r}\xi(x)\,dM_e(x)\right\} \quad (21)$$

where

$$P(r_1) = \int_{x=0}^{r_1}\xi(x)\,dM_e(x) = \frac{r_1\,\xi(r_1)\,v^2(r_1)}{G} = \text{constant} \quad (22)$$

This shows that we can normalise our fit to the rotation curve at an arbitrary point, r_1, and continue to work our way outwards. This is useful for galaxies where we do not have good data for the inner regions. We can simply start at a point some way out from the centre. This has no effect on our determination of the shape of the $\xi(r)$ function beyond the normalisation point.

4.4 The linear approximation apparent in the bottom left panels means we can express the $\xi(r)$ function as

$$\frac{\xi(r)}{\xi_0} = \left\{\frac{r_0}{r}\right\}^{\alpha} \quad (23)$$

where ξ_0 is the value of the ξ-function at some normalisation distance, r_0. The slope of the line in the bottom left panel is negative with a value of order -1. This means that the α exponent in equation (23) is positive with a value of order +1.

4.5 Equation (23) is clearly divergent at the origin, where the ξ function becomes infinite. However, we are working numerically and do not have a data point at the origin. For the analysis we set an average of ξ=1000 across the first interval, and ξ=500 at the first data point. When constructing our predicted rotation curve, we assume the average value of ξ across the first interval is double its value at the first data point. In this way the divergence of ξ at the origin is not a problem.

4.6 Substituting equation (23) into equation (13) gives

$$v^2(r) = \frac{G}{r}\, r^{\alpha} \int_{x=0}^{r} \frac{1}{x^{\alpha}}\, dM_e(x) = \frac{G}{r} \int_{x=0}^{r} \left\{\frac{r}{x}\right\}^{\alpha} dM_e(x) \qquad (24)$$

We note that, because there are $\xi(r)$ terms in both the numerator and denominator of equation (13), equation (24) does not contain ξ_0 or r_0; they cancel out. For the SPARC galaxies it is found that α lies in the range $+0.5 \leq \alpha \leq +1.8$.

4.7 It is interesting to compare equation (24) with equation (12), repeated below, for the expected velocity

$$u^2(r) = \frac{G}{r} \int_{x=0}^{r} dM_e(x) \qquad (12)$$

The similarities and differences are strikingly apparent.

4.8 We do not expect equation (24) to fit the entire rotation curve, just that section where there appears to be a linear relation between $log(\xi)$ and $log(r)$. In particular we expect departures to occur at large distances because, at some point, the rotational velocity should return to being proportional to the inverse root of the distance, $v \propto 1/\sqrt{r}$. Also, we expect departures at the origin as discussed in 4.5 above.

4.9 We have arrived at equation (24) from the observational data of disk galaxies in the SPARC catalogue and the assumption that equation (13) holds. We did not expect to come up with such a simple relation with only one adjustable parameter. There is a different value of the α-parameter for every galaxy; α is not a universal constant. The rotation curves for different galaxies are different simply because the mass distributions, $dM_e(x)$, are different (and because the energy scale variations, as characterised by α, are different).

5 Fitting procedure

5.1 In this section we look at how we use equation (24) to fit the observed rotation curves of SPARC galaxies.

5.2 When we come to fit the observed rotation curve using equation (24) with our power law for the ξ-function, equation (23), we have just two adjustable parameters:

(a) Υ, the mass-to-light ratio of the stellar disk. Typically, Υ lies in the range 0.3 to 1.0. By varying Υ we vary the distribution of the stellar mass across the galaxy and so vary the $\boldsymbol{dM(x)}$ term in equation (24).

(b) the exponent, $\boldsymbol{\alpha}$, of the power law relation for the ξ-function, as defined by equation (23). Typically, $\boldsymbol{\alpha}$ lies in the range +0.5 to +1.8.

5.3 It is a straightforward matter to use a brute force approach and carry out a grid search for the best fit.

5.4 We start by choosing a value for the mass-to-light ration, Υ, in the range 0.20 to 2.00. Equation (16) then gives us the expected rotational velocity using the values in the SPARC catalogue.

5.5 Next, we by derive the mass distribution, $\boldsymbol{dMe}(\boldsymbol{x})$, by inverting equation (12); essentially using equation (17) for the expected rotational velocity as given in step 5.4 above.

5.6 We now choose a value for the exponent, $\boldsymbol{\alpha}$, in the range +0.20 to +2.10, and calculate our prediction for the observed velocity using equation (24).

5.7 We define the fit as the sum of the squares of the differences between our predicted velocity and the observed velocity in the SPARC catalogue.

5.8 The best fit is simply the numerically smallest value of the fit across our grid of values.

5.9 We do not blindly accept this but plot out the rotation curve of the SPARC values and our predicted values. We then inspect the plots to check that our predicted curve does indeed fit the observations. In most cases the fit is quite acceptable, and we can end the process there.

5.10 However, occasionally we have a troublesome galaxy, and the visual inspection shows that something is not right. In these cases, we can delete some of the SPARC data points and attempt to fit a reduced part of the rotation curve. It is invariably points in the outer part of the galaxy where we have to delete points. But this is exactly where we expect our adoption of equation (24) to break down.

5.11 For most galaxies the best fit is clear and unambiguous. There is usually a unique choice of Υ and α that gives the best result.

5.12 A few galaxies have a central bulge with its own mass-to-light ratio. These are fitted by treating this mass-to-light ratio as an additional parameter and extending the grid search to cover it as well.

5.13 We should stress that in using equation (24) to fit the observed rotation curves we are using the actual mass distribution for the galaxy as inferred from observations. There is no approximation or assumed functional form; we simply plug in the actual masses as given by the SPARC data.

5.14 As an example we can consider galaxy NGC 2403, shown earlier in one of the panels. The grid search results in the mass-to-light ratio, Υ=0.45, and the exponent, α=+1.02 (i.e. slope=-1.02). With these two values we can construct our predicted rotation curve. We start at the innermost data point, add in the galaxy's actual mass increment, and integrate our way outwards. The fitted rotation curve, the red line in the bottom right panel, works all the way from the innermost data point at 0.2kpc out to 21kpc. There are bumps and kinks in the observed rotation curve that are not reproduced in the fitted curve. Nevertheless, the overall fit, while not perfect, is astonishing.

6 Hybrid test

6.1 Stacy McGaugh (2018) has pointed out that, given a rotation curve and a mass distribution, it is always possible to find a dark matter halo that fits the data. For example, a good dark matter fit can be found using the rotation curve of NGC 2403 and the mass distribution of UGC 128.

6.2 The panels on the next page show what happens when we try this same test with our fitting procedure. The data for NGC 2403 and UGC 128 are mapped onto a 2kpc grid and only extend to 20kpc (the limit of NGC 2403). The hybrid panel can be compared to the individual panels for the two galaxies displayed earlier.

6.3 The top left panel shows the observed rotation curve of NGC 2403 (black diamonds) and expected rotation curve for the mass distribution of UGC 128 (blue line).

6.4 The top right panel shows the cumulative mass distributions matching the velocity distributions of the top left panel.

6.5 The bottom left panel shows the ξ-function. A modest linear fit can be found for part of the data. However, it does not look like any of the plots for actual galaxies.

6.6 The bottom right panel shows the best fit we can obtain (red line). The mass-to-light ratio has to be set at the unphysically high value of Υ=6.0. Even with this the fit is bad and shows large systematic differences from the actual rotation curve.

6.7 No satisfactory fit can be found. Overall, we should be pleased with this result. It shows that our procedures cannot be fooled by a hybrid galaxy; not in the same way that dark matter can be fooled.

Hybrid1

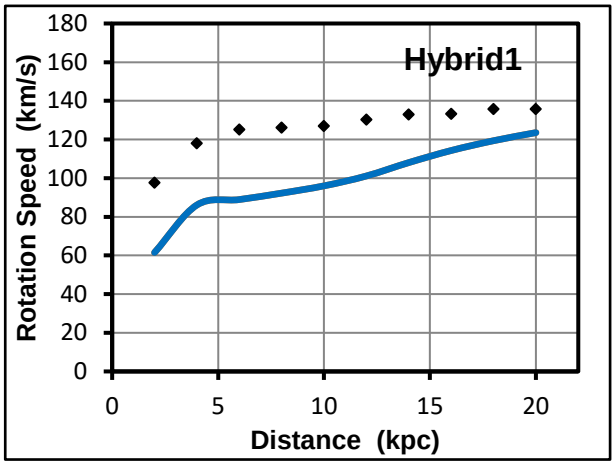

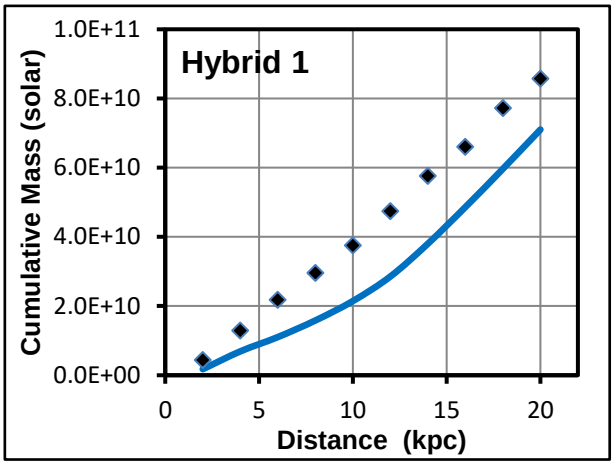

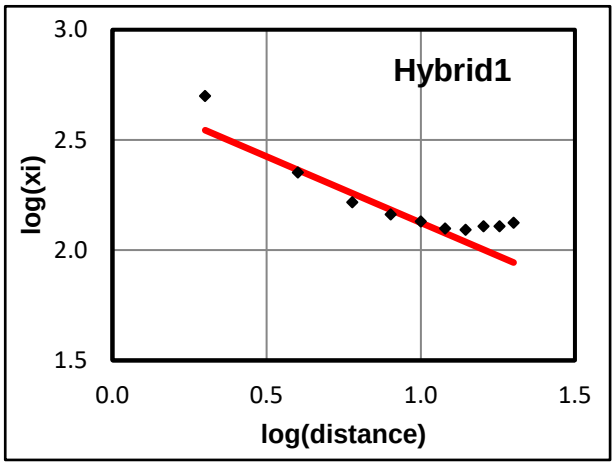

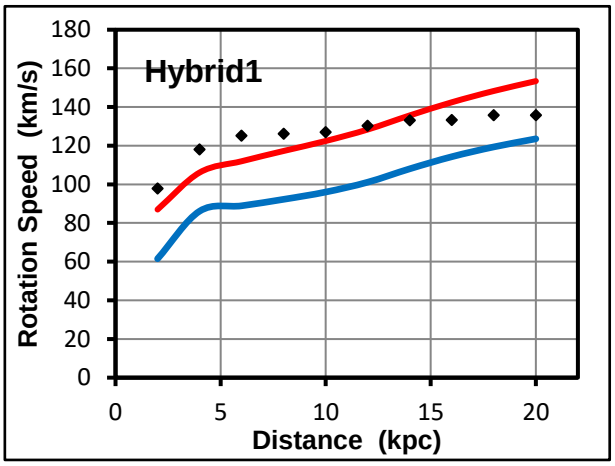

Top left: rotation curve: black diamonds NGC 2403; blue line UGC 128.
Top right: cumulative mass: black diamonds NGC 2403; blue line UGC 128
Bottom left: ξ-function
Bottom right: fitted rotation curve

Fit parameters

ϒ, M-to-L	6.00
ξ, slope	-0.60
DM factor	0.2
Fit quality	bad

Hybrid test showing what happens when we use the rotation curve of NGC 2403 and the mass distribution of UGC 128. No satisfactory fit can be found.

7 Correlations

7.1 We can look at the results of applying the above analysis to the SPARC galaxies and see if there are correlations between the α exponent and any other parameter.

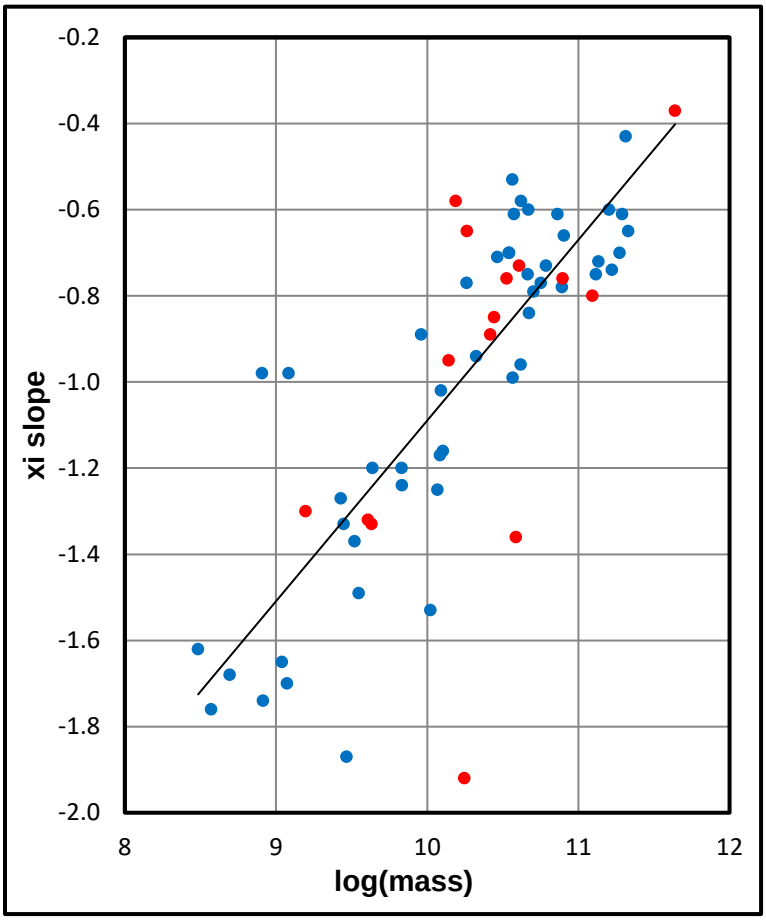

Figure 1. Plot of the slope of the ξ-function against galaxy mass. The α exponent is the negative of this slope. Blue points are good fits; red points poor fits.

7.2 Figure 1 shows the plot of the slope of the ξ-function (that describes the energy scale variation) against galaxy mass, for 64 galaxies in the SPARC catalogue. This slope is obtained from the bottom left panels of the galaxy displays. The α exponent, in equation (24), is the negative of this slope. The blue points are galaxies where there is a good fit to the observed rotation curve; the red points are poor fits. There is a clear correlation between galaxy mass and the α exponent, as indicated by the straight line fit. The correlation coefficient (for the blue points) has a value of 0.75, indicating a reasonably good correlation.

7.3 We are now in the position where we can generate the observed rotation curve from observations of the mass distribution alone. Figure 1 gives us an estimate for the value of the α exponent from the total mass of the galaxy. Equation (24) then gives the observed rotation curve from the mass distribution. There is no need to add in any dark matter.

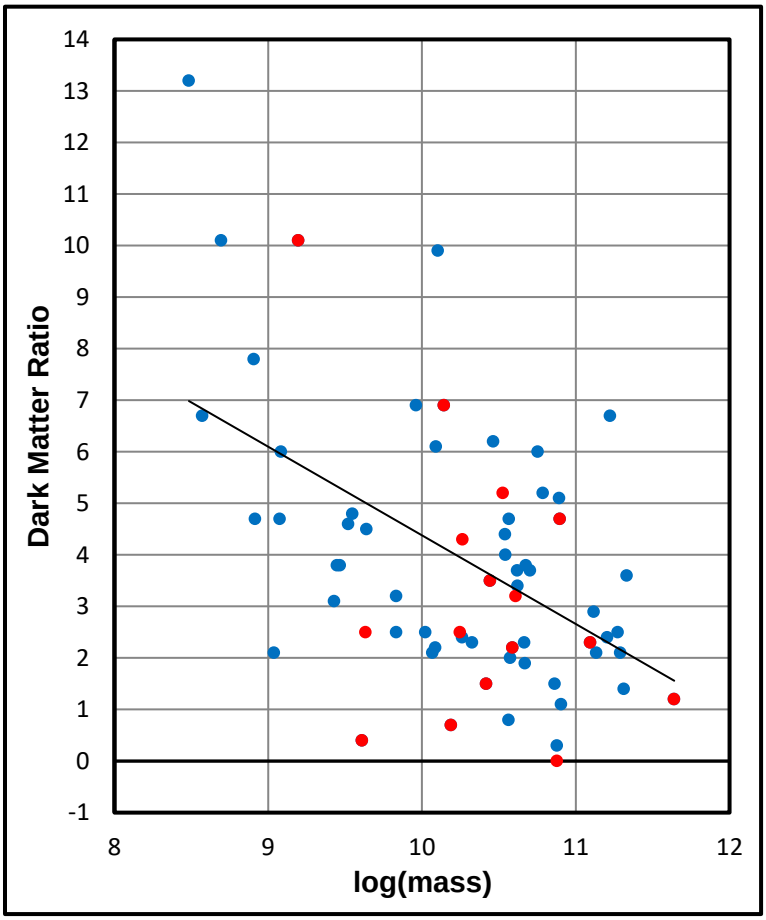

Figure 2. Plot of dark matter ratio against galaxy mass. Blue points are good fits; red points poor fits.

7.4 Figure 2 shows the plot of dark matter ratio, as given by equation (24), against the mass, for 64 galaxies in the SPARC catalogue. The blue points are galaxies where there is a good fit to the observed rotation curve; the red points are poor fits. There is a weak correlation between dark matter ratio and the galaxy mass, as indicated by the straight line fit. The correlation coefficient (for the blue points) has a value of 0.26, indicating a weak correlation.

7.5 In terms of dark matter: the weak correlation in Figure 2 suggests that massive galaxies have little dark matter and low mass galaxies have a lot of dark matter. However, our overall position is that dark matter does not exist.

7.6 The average value of the dark matter ratio in Figure 2 is 3.8. This is some way away from the usually quoted value of 5 for the ratio of dark matter to normal matter in galaxies. The value would be even lower if we left out the few high value galaxies that somewhat skew the ratio.

7.7 Figures 1 & 2 are based on 64 galaxies from the 175 in the SPARC catalogue. No deliberate selection criteria have been used; essentially, we worked with all the NGC galaxies. We are continuing to plough our way through the entire catalogue, but do not expect any changes to Figures 1 & 2 to arise.

8 Limiting cases

8.1 We noted earlier that the linear behaviour of the logarithm of the ξ-function in the bottom left panels was unexpected. In this section we look at a couple of limiting scenarios that go some way to explaining this.

8.2 First we consider the somewhat artificial case of a central mass, $\boldsymbol{M_0}$, and a flat rotation curve with constant velocity, $\boldsymbol{v_c}$. Equation (5) reduces to

$$\boldsymbol{v_c^2} \;=\; \frac{\boldsymbol{G}}{\boldsymbol{r}}\,\frac{\boldsymbol{1}}{\boldsymbol{\xi(r)}}\;\boldsymbol{\xi_0\,M_0} \tag{25}$$

This can be written as

$$\boldsymbol{\xi(r)} = \left\{\frac{\boldsymbol{G\,\xi_0\,M_0}}{\boldsymbol{v_c^2}}\right\}\frac{\boldsymbol{1}}{\boldsymbol{r}} = \{\boldsymbol{\xi_0\;r_o}\}\,\frac{\boldsymbol{1}}{\boldsymbol{r}} \tag{26}$$

or

$$\frac{\boldsymbol{\xi(r)}}{\boldsymbol{\xi_0}} = \left\{\frac{\boldsymbol{r_0}}{\boldsymbol{r}}\right\} \tag{27}$$

This is equation (23) with the α-parameter having the value $\boldsymbol{\alpha}$=+1.0.

8.3 So we should, perhaps, have anticipated the power law relationship between the ξ-function, $\boldsymbol{\xi(r)}$, and distance, $\boldsymbol{r}$. We also note that the observed range of the $\boldsymbol{\alpha}$-parameter from +0.5 to +1.8 spans this limiting value of +1.0.

8.4 The other limiting case is the behaviour at large distances. At some distance, R, the galaxy ends, and the mass of the galaxy converges to some final value. Also, in equation (13), the increments in mass, $\boldsymbol{dM_e(x)}$, are weighted with the ξ-function, which we now know decreases with distance. So, the inner parts of the galaxy are weighted more heavily than the outer regions. Together these mean

$$\int_{\boldsymbol{x=0}}^{\boldsymbol{R}} \boldsymbol{\xi(x)\,dM_e(x)} = \;\boldsymbol{M_T}\; = \text{ constant} \tag{28}$$

at some distance R.

8.5 Also we do not expect the ξ-function to continue decreasing for ever, but to reach some terminal value, $\boldsymbol{\xi_T}$, at large distances. For some SPARC galaxies the observed log($\boldsymbol{\xi}$) vs log($\boldsymbol{r}$) plots do show signs of levelling off at large distances, indicating the ξ-function is tending towards a terminal value. In these circumstances, equation (13) becomes

$$\boldsymbol{v^2(r) = \left\{\frac{G\,M_T}{\xi_T}\right\}\frac{1}{r}} \qquad (29)$$

where the bracketed term on the right-hand side is constant. We are now back with the rotation curve declining with the inverse root of the distance. So, at large distances, we have the normal fall off for Newtonian gravity; this is exactly what we want to see.

8.6 So we expect the rotation curve to be covered by equation (24) out to some large distance where it transitions to equation (29). Where this transition occurs depends on the observed data; we cannot predict this point (at the present time).

8.7 The effective terminal mass, $\boldsymbol{M_T}$, in equation (28) is much greater than the galaxy's actual mass. This means at large distances the galaxy behaves gravitationally as if it had a much greater mass; typically at least 5 times greater. This effect applies to other scenarios where gravity is involved and explains why dark matter is not needed in those scenarios. These scenarios are covered in other papers in this series.

9 Theoretical consideration

9.1 We started with the theoretical conjecture that the energy scale can vary from location to location. This gave us equation (13). Analysis of the SPARC observational data then led directly to equation (24).

9.2 Currently we have no theoretical understanding as to why equation (24) should hold, even as an approximation:

$$v^2(r) = \frac{G}{r}\, r^{\alpha} \int_{x=0}^{r} \frac{1}{x^{\alpha}}\; dM_e(x) \tag{24}$$

9.3 Equation (24) can be integrated by parts to give

$$v^2(r) = \frac{G\, M_e(r)}{r} + \frac{1}{r}\, r^{\alpha} \int_{x=0}^{r} \left\{\frac{G\, M_e(x)}{x}\right\} \frac{\alpha}{x^{\alpha}}\; dx \tag{30}$$

9.4 For our exponential disk with effective mass, $M(x)$, the gravitational potential, $\varphi(x)$, at x is given by:

$$\varphi(x) = \frac{G\, M_e(x)}{x} \tag{31}$$

9.5 This means we can write equation (24) in terms of the gravitational potential:

$$v^2(r) = \varphi(r) + \frac{\alpha}{r} \int_{x=0}^{r} \left\{\frac{r}{x}\right\}^{\alpha} \varphi(x)\; dx \tag{32}$$

9.6 We have no further insights into equations (24) or (32): but other researchers might.

10 Acceleration

10.1 If we divide equations (12) and (24) by the radial distance, $\boldsymbol{r}$, we end up with the radial acceleration

$$\boldsymbol{g_u(r)} = -\frac{\boldsymbol{u^2(r)}}{\boldsymbol{r}} = -\frac{\boldsymbol{G}}{\boldsymbol{r^2}}\int_{\boldsymbol{x=0}}^{\boldsymbol{r}} \boldsymbol{dM_e(x)} \tag{33}$$

$$\boldsymbol{g_v(r)} = -\frac{\boldsymbol{v^2(r)}}{\boldsymbol{r}} = -\frac{\boldsymbol{G}}{\boldsymbol{r^2}}\int_{\boldsymbol{x=0}}^{\boldsymbol{r}} \left\{\frac{\boldsymbol{r}}{\boldsymbol{x}}\right\}^{\boldsymbol{\alpha}} \boldsymbol{dM_e(x)} \tag{34}$$

10.2 McGaugh et al (2016) have found a universal relation between $\boldsymbol{g_u(r)}$ and $\boldsymbol{g_v(r)}$ for disk galaxies; the so-called radial acceleration relation. Researchers, more able than us, may be able to derive this mathematically from equations (33) & (34). We would expect a new relation between McGaugh's curve and our $\boldsymbol{\alpha}$ exponent.

10.3 The modified gravity hypothesis (MOND) also works with acceleration and suggests that Newton's law of gravity takes a different form at the very low accelerations encountered in disk galaxies. Again, other researchers may be able to arrive at the MOND equation from equations (33) & (34).

10.4 We leave these two ideas to researchers more able than ourselves.

11 Cosmological connection

11.1 Despite what we have said earlier about not understanding equations (23) & (24), we notice a similarity with the equations of cosmic dynamics as set out in Ryden (2017).

11.2 The fluid equation (Ryden, equation 4.44) is

$$\dot{\varepsilon} + 3\frac{\dot{a}}{a}(\varepsilon + P) = 0 \tag{35}$$

where ε is the energy density; a the scale factor; P the pressure; dots represent differentiation with respect to time.

11.3 The equation of state (Ryden, equation 4.55) is

$$P = w\,\varepsilon \tag{36}$$

where w is a dimensionless number.

11.4 These lead to (Ryden, equation 5.9)

$$\frac{\varepsilon}{\varepsilon_0} = \left(\frac{a}{a_0}\right)^{-3(1+w)} \tag{37}$$

where, by convention, $a_0 = 1$.

11.5 This can be compared directly to our equation (23)

$$\frac{\xi(r)}{\xi_0} = \left\{\frac{r}{r_0}\right\}^{-\alpha} \tag{23}$$

11.6 Equations (37) and (23) have an identical form.
The left-hand sides of both equations relate to energy.
The right-hand sides of both equations relate to distance.

11.7 This connection is somewhat speculative, and we leave further investigations to others.

12 Summary

12.1 The conjecture that the energy scale can vary from location to location leads directly to equation (13) for the rotational velocity of a disk galaxy:

$$v^2(r) = \frac{G}{r}\frac{1}{\xi(r)}\int_{x=0}^{r}\xi(x)\,dM_e(x) \tag{13}$$

where $\xi(r)$ is the function that describes the energy scale variation.

12.2 The application of equation (13) to the data in the SPARC catalogue leads to the $\xi(r)$ function being found to have the simple form of equation (23):

$$\frac{\xi(r)}{\xi_0} = \left\{\frac{r_0}{r}\right\}^{\alpha} \tag{23}$$

i.e. $\xi(r)$ is simply the inverse distance raised to some (small) power.

12.3 Equation (23) drops out of the data in the SPARC catalogue. It is an observational result. Its simple form was not anticipated at all.

12.4 Equations (13) and (23) combine to give equation (24) for the observed rotation curve.

$$v^2(r) = \frac{G}{r}\int_{x=0}^{r}\left\{\frac{r}{x}\right\}^{\alpha}dM(x) \tag{24}$$

12.5 Good fits to the observed rotation curves of SPARC galaxies are found using equation (24). The only adjustable parameter is the α exponent, which is found to take values in the range +0.5 to +1.8.

12.6 It is presumed that there is some deeper underlying significance to these equations; this significance is not fully understood at the present time.

13 Discussion

13.1 The conjecture that the energy scale can vary from location to location led us to our starting point of equation (13). This conjecture also means that the gravitational constant, G, is an absolute constant and has the same value everywhere. Also, the equivalence principle holds with the gravitational mass being equal to the inertial mass everywhere. For example: identical A-type stars can exist equally well in the galaxy centre as in the outer spiral arms, despite the energy scale having different values. These and other matters are discussed in other papers in this series.

13.2 Whether you believe in dark matter, energy scale variations, or rolling fudge factors, the existence of equation (24) and its ability to reproduce the observed rotation curves of disk galaxies is both surprising and astonishing. And all with only one adjustable parameter, which can itself be estimated knowing just the total mass of the galaxy.

13.3 Equation (24) is an observational result. It arises from applying equation (13) to the data in the SPARC catalogue. It is supported by the fact that, using it, good fits can be found to the rotation curves of SPARC galaxies.

13.4 The rotation curves can be reproduced using equation (24) and the observed distribution of baryonic mass in the galaxies. There is no need to add in any additional mass in the form of dark matter.

13.5 This paper demonstrates that there is no requirement for dark matter to exist in disk galaxies.

13.6 It should be possible to apply the analysis presented in this paper to certain clusters of galaxies. The observed mass distribution may be available from observations of the galaxy members and X-ray emissions from the hot gas. The expected mass distribution may be available from the dynamics of galaxy members and gravitational lensing.

13.7 Other papers in this series show how variations in the energy scale can explain all other scenarios where dark matter is invoked, including: cosmic microwave background; baryon acoustic oscillations; structure formation; galaxy collisions; galaxy clusters; gravitational lensing.

14 References

Binney, J; Tremaine, S. "Galactic Dynamics" 2nd Ed. (2008). Princeton University Press.

JoKe1. (2015). "On the variation of the energy scale: An alternative to dark matter". **www.varensca.com**

JoKe2. (2015). "On the variation of the energy scale 2: Galaxy rotation curves". **www.varensca.com**

JoKe3. (2015). "On the variation of the energy scale 3: Parameters for galaxy rotation curves". **www.varensca.com**

JoKe23. (2019). "On the variation of the energy scale 23: SPARC galaxy rotation curves". **www.varensca.com**

Lelli, L; McGaugh SS; Schombert JM. (2016). "SPARC: Mass Models for 175 Disk Galaxies with Spitzer Photometry and Accurate Rotation Curves".
arXiv.1606.09251
The Astronomical Journal; volume 152; issue 6.

McGaugh, SS. (2018). "Hypothesis testing with gas rich galaxies". November 2018. https://tritonstation.wordpress.com

McGaugh SS; Lelli, F; Schombert JM. (2016). "The Radial Acceleration Relation in Rotationally Supported Galaxies".
arXiv.1606.05917

Ryden, B. "Introduction to Cosmology" 2nd Ed. (2017). Cambridge University Press.